ACCOUNTS of chemical research

Article

pubs.acs.org/accounts

Electron Transfer, Decoherence, and Protein Dynamics: Insights from Atomistic Simulations

Published as part of the Accounts of Chemical Research special issue "Protein Motion in Catalysis".

Christophe Narth,[†] Natacha Gillet,[‡] Fabien Cailliez,[‡] Bernard Lévy,[‡] and Aurélien de la Lande*[,‡]

[†]Laboratoire de Chimie Théorique, CNRS UMR 7616, Université Pierre et Marie Curie, case courrier 137. 4, Place Jussieu, 75252 Cedex 05 Paris, France

[‡]Laboratoire de Chimie-Physique, CNRS UMR 8000, Université Paris Sud, Bâtiment 349 - Campus d'Orsay. 15, avenue Jean Perrin, 91405 Cedex Orsay, France

Supporting Information

CONSPECTUS: Electron transfer in biological systems drives the processes of life. From cellular respiration to photosynthesis and enzymatic catalysis, electron transfers (ET) are chemical processes on which essential biological functions rely. Over the last 40 years, scientists have sought understanding of how these essential processes function in biology. One important breakthrough was the discovery that Marcus theory (MT) of electron transfer is applicable to biological systems. Chemists have experimentally collected both the reorganization energies (λ) and the driving forces ($\Delta G°$), two parameters of Marcus theory, for a large variety of ET processes in proteins. At the same time, theoretical chemists have developed computational approaches that rely on molecular dynamics and quantum chemistry calculations to access numerical estimates of λ and $\Delta G°$.

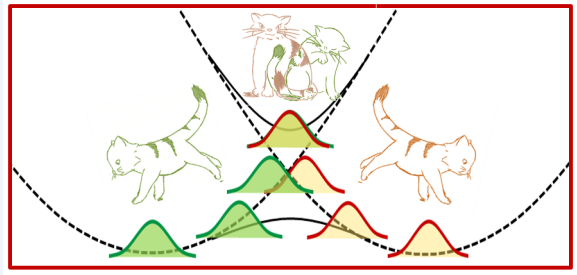

Coherent Schrödinger cat ?

Yet another crucial piece in determining the rate of an electron transfer is the electronic coupling between the initial and final electronic wave functions. This is an important prefactor in the nonadiabatic rate expression, since it reflects the probability that an electron tunnels from the electron donor to the acceptor through the intervening medium. The fact that a protein matrix supports electron tunneling much more efficiently than vacuum is now well documented, both experimentally and theoretically. Meanwhile, many chemists have provided examples of the rich physical chemistry that can be induced by protein dynamics.

This Account describes our studies of the dynamical effects on electron tunneling. We present our analysis of two examples of natural biological systems through MD simulations and tunneling pathway analyses. Through these examples, we show that protein dynamics sustain efficient tunneling.

Second, we introduce two time scales: τ_{coh} and τ_{FC}. The former characterizes how fast the electronic coupling varies with nuclear vibrations (which cause dephasing). The latter reflects the time taken by the system to leave the crossing region. In the framework of open quantum systems, τ_{FC} is a short time approximation of the characteristic decoherence time of the electronic subsystem in interaction with its nuclear environment. The comparison of the respective values of τ_{coh} and τ_{FC} allows us to probe the occurrence of non-Condon effects. We use *ab initio* MD simulations to analyze how decoherence appears in several biological cofactors. We conclude that we cannot account for its order of magnitude by considering only the atoms or bonds directly concerned with the transfer. Decoherence results from contributions from all atoms of the system appearing with a time delay that increases with the distance from the primarily concerned atoms or bonds. The delay and magnitude of the contributions depend on the chemical nature of the system.

Finally, we present recent developments based on constrained DFT for efficient and accurate evaluations of the electronic coupling in *ab initio* MD simulations. These are promising methods to study the subtle fluctuations of the electronic coupling and the mechanisms of electronic decoherence in biological systems.

BIOLOGICAL ELECTRON TRANSFERS

In this Account, we focus on electron transfers (ETs) in biological systems. In that medium, ETs take place between donor and acceptor groups of atoms (hereafter, respectively, denoted D and A) including organic compounds (e.g., quinones, flavins, pheophytins, tryptophan, and tyrosine) or transition metal complexes (e.g., blue copper centers, iron–sulfur clusters, and hemes). Electron transfers are seen, for example, in the cellular respiratory chain where electrons are transported from protein to protein,[1] in enzymatic catalysis where numerous enzymes need to be supplied by electrons to

Received: July 31, 2014
Published: March 2, 2015

DOI: 10.1021/ar5002796
Acc. Chem. Res. 2015, 48, 1090–1097

fulfill their biological activity, or in DNA.[2,3] Although of paramount importance in biology, we will not deal in this Account with proton-coupled electron transfers.[4,5]

The chemical physics of ET is now well understood and will be recalled here very briefly. We introduce two electronic states (φ_A, φ_D) corresponding to quantum states where the excess of charge is localized either on D or on A. In fact φ_A and φ_D are not eigenvectors of the electronic Hamiltonian ($\hat{H}_{el}$) but rather diabatic states. By construction, they are coupled one to another through the electronic Hamiltonian ($H_{DA} = \langle\varphi_A|\hat{H}_{el}|\varphi_D\rangle \neq 0$).[6] When the electronic coupling is weak, ET rates can be estimated in the high temperature limit by the nonadiabatic Marcus theory expression (semiclassical limit of the perturbative Fermi Golden Rule):[7]

$$k_{DA} = \frac{2\pi}{\hbar}\frac{1}{\sqrt{4\pi\lambda k_B T}}H_{DA}{}^2 \exp\left(-\frac{(\lambda + \Delta G^\circ)^2}{4\lambda k_B T}\right) \quad (1)$$

λ is the reorganization energy and ΔG° is the free energy of the reaction. Both can be estimated by microscopic simulations, and we refer the reader to some reviews on these aspects of ET.[8,9] We will rather focus on the electronic coupling term (H_{DA}). Tunneling is probably the most accepted physicochemical mechanism for accounting for electron transfer from D to A.[10−12] The intervening medium extends the range of the electronic function φ_D (φ_A) beyond the donor (acceptor) site toward the acceptor (donor). Consequently the electronic coupling is larger in a biomolecule than in vacuum for a given D−A distance.[13] Models derived from first principles such as the tunneling pathways model[14] or the interatomic current model[15] have been established to relate the composition of the intervening medium to its capability to support tunneling. An interesting feature of this mechanism is the possible occurrence of interferences among competitive pathways.[16,17]

PROTEIN DYNAMICS AND EFFICIENT TUNNELING PATHWAYS

Numerical simulations can bring valuable insights about how protein matrices support tunneling in natural biological systems. A usual strategy is to carry out molecular dynamics simulations and to evaluate the electronic coupling along the trajectory.[17−24] We have applied this strategy to intraprotein ET like in peptidylglycine α-hydroxylating monooxygenase,[25,26] flavohemoglobin,[27] or cryptochromes,[28] as well as to interprotein ET.[29] We reprise here two of these studies.

The first example is provided by the pair of proteins methylamine dehydrogenase (MADH) and amicyanin (Am) from *Paracoccus denitrificans*.[29] There have been extensive studies of the ET from the tryptophan tryptophylquinone (TTQ) cofactor of MADH to the blue copper center of Am (Figure 1).[30]

We completed classical molecular dynamics simulations of 40 ns duration, coupled to the evaluation of H_{DA} by the empirical pathway model.[14] The results indicated that the interstice between the two proteins is ideally sized to host two water molecules in adequate position to sustain efficient tunneling pathways. Moreover during MD simulations of mutated enzymes (targeting Met 51), water molecules from the bulk can penetrate more easily to the protein interstice, in turn weakening the most efficient tunneling pathways. The decay of ET rates in mutated systems, which results from smaller average squared electronic couplings, could account for the rate decay observed experimentally.[31] Some hydrophobic residues of

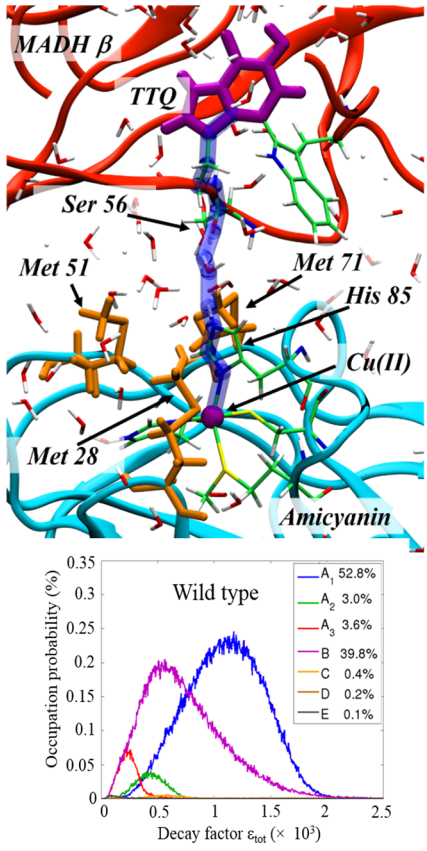

Figure 1. (top) Dominant water mediated pathway mediating electron transfer from the TTQ cofactor of MADH (in red ribbons) to the cupric cation of amicyanin (in blue ribbons). The pathway involves one water molecule hydrogen bonded to MADH Ser 56 and Am His 95. (bottom) Distribution of the pathway types for wild-type MADH/amicyanin pair.[29] Adapted with permission from ref 29. Copyright 2010 National Academy of Sciences of the United States of America.

amicyanin (Met 51, 71, and 28) surrounding the cavity seem to play a role of breakwater, protecting the water-mediated pathways from the bulk of water molecules. Overall our data suggested that surface residues dynamically organize water bridges to enhance electron transfer from MADH to amicyanin.

A second example deals with the ultrafast electron transfer in *Arabidopsis thaliana* cryptochromes (*At*Cry). Cry are flavoproteins encountered in most vegetal and animal species, playing the role of blue-light receptors in plants and in vertebrates.[32] Upon excitation, an oxidized flavin adenine dinucleotide (FAD) cofactor undergoes a reduction by abstraction of an electron from a nearby tryptophan residue (Trp 400 in Figure 2). This ET triggers a cascade of electron/hole transfers along a triad of tryptophan residues, ultimately leading to $FADH^\bullet$.[33] Experimental evidence demonstrates that ATP binding increases the yield of formation of $FADH^\bullet$. It was proposed that ATP binding induces a pK_a shift of aspartic acid 396 (the putative proton donor to FAD^-).[34] We estimated the rates of ET from Trp 400 to FAD* (step 1 in Figure 2) by means of MD simulations coupled to time-dependent density functional theory (TD-DFT) calculations.[28] We considered four systems: *At*Cry in the presence or absence of ATP and Asp 396 being protonated or not. In all cases, ET was found to be limited by H_{DA}. When ATP was present and Asp 396 was protonated, FAD remained in close contact with Trp 400, thereby enhancing H_{DA} and consequently the ET rate. In contrast,

DOI: 10.1021/ar5002796
Acc. Chem. Res. 2015, 48, 1090−1097

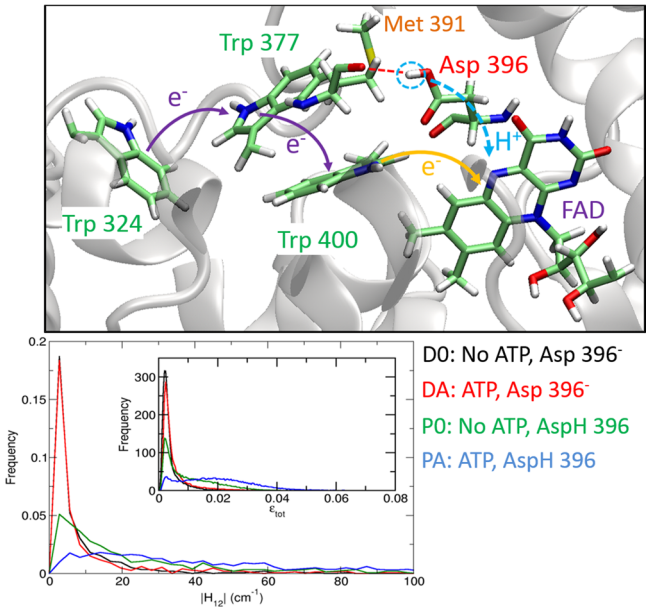

Figure 2. Ultrafast electron transfer within plant cryptochrome. (top) Molecular view of the photoactive site. After excitation of FAD in the S1 state, an electron is transferred from Trp 400 to FAD*. (bottom) Histograms of $|H_{12}|$ calculated from TD-DFT calculations The inset graph shows histograms of the decay factor, ε_{tot}, from a pathway model analysis. Adapted with permission from ref 28. Copyright 2014 American Chemical Society.

deprotonation of Asp 396 and absence of ATP introduce flexibility to the photoactive site prior to FAD excitation, with the consequence of increased FAD−Trp 400 distance and diminished tunneling rate by almost 2 orders of magnitude. This study illustrates how the binding of a cofactor near the photoactive site of a protein can indirectly favor a productive photoinduced ET by modulation of H_{DA}.[28]

These studies based on classical MD simulations, as well as many others,[18,21−23,35−38] indicate that proteins dynamics may have a direct impact on macroscopic ET rates through modulation of $\langle H_{DA}^2 \rangle$. The examples of the MADH/amicyanin pair and of the *At*Cry are especially striking, suggesting that evolution favored the selection of particularly strong tunneling pathways

TOWARD A COMPREHENSIVE UNDERSTANDING OF ELECTRONIC DECOHERENCE

Introductive Theoretical Background

In the previous examples, the relationships between electronic couplings and ET rates were sought in the context of eq 1, therefore assuming constant H_{DA} when the system visits a region of quasi-degeneracy. Actually since H_{DA} can be extremely sensitive to small changes in the D-bridge-A structure, this hypothesis might not be always valid.[39] Two characteristic time scales are customarily introduced to discuss the eventuality of such non-Condon effects.[40] On one hand, it is necessary to evaluate how fast H_{DA} fluctuates with nuclear motions. The latter can lead to dephasing among ET pathways. The time scale for this type of coherence loss (τ_{coh}) can be estimated from the characteristic decay time of the normalized autocorrelation function of H_{DA} ($C^n_{H_{DA}}(t) = \langle H_{DA}(t)H_{DA}(0)\rangle / \langle H_{DA}(0)^2\rangle$). A second time is called the characteristic Franck−Condon time (τ_{FC}). It reflects the time taken by the system to escape the Franck−Condon region of allowed electronic transition. Onuchic and co-workers proposed to relate τ_{FC} to the reorganization energy (λ).[41] This relationship intuitively stems from the fact that the larger the reorganization energy, the larger the angle made by the Marcus parabola at the crossing point, and therefore the faster the nuclear wave packets will escape the FC region. With typical values of λ ranging from 0.1 to 1.5 eV, τ_{FC} is predicted to fall in a time window of 1−10 fs.

$$\tau_{FC} \approx \frac{\hbar}{\sqrt{2\lambda k_B T}} \tag{2}$$

Alternatively, Prezhdo and Rossky proposed an expression (eq 3) relating τ_{FC} to the difference of forces (ΔF_{12}) felt by the nuclei on the two potential energy surfaces PES and the widths of the nuclear wave packets (a_n).[42]

$$\tau_{FC} = \left[\left\langle \sum_n \frac{1}{2a_n\hbar^2} (\Delta F_{12})^2 \right\rangle_T \right]^{-1/2} \tag{3}$$

In eq 3, $\langle ... \rangle_T$ denotes a canonical average at temperature T. Actually eq 3 was derived by these authors as a short time approximation to the characteristic electronic decoherence time of the system. In the theory of open quantum systems, decoherence refers to the processes by which the off-diagonal elements of a reduced density matrix of a system decay to zero because of interactions with its environment.[42,43]

When $\tau_{coh} \gg \tau_{FC}$, H_{DA} can be considered as constant each time the system visits a region of degeneracy, and a separation of the electronic and nuclear factors like in eq 1 holds. On the contrary if $\tau_{coh} \ll \tau_{FC}$, this separation is not possible, which may lead to interesting non-Condon effects like inelastic interactions between the tunneling electron and bridge vibrations.[18,40] Kinetic models for dealing with ET that depart from the Condon approximation have been devised by various groups.[44−46]

Numerical Simulations of Electronic Decoherence of Biological Cofactors

Numerical simulations can again shed light on the molecular mechanisms that determine τ_{coh} and τ_{FC}. For example, Skourtis et al. pointed out in a series of Ru-modified azurin derivatives the role played by valence angles in triggering fluctuations of H_{DA} eventually through dihedral angle and hydrogen bond length fluctuations. They found a range of 20−56 fs for τ_{coh}.[47] Values of similar order were found by Nishioka et al. for ET between a bacteriopheophytin and a quinone cofactor of the photoreactive center of *Rhodobacter sphaeroides*.[45] Troisi et al. obtained τ_{coh} of 0.1 ps for ET in C-clamp molecules in different solvents.[21] Regarding τ_{FC}, Lockwood et al. reported an investigation in ruthenium modified protein by means of classical MD simulations, predicting $\tau_{FC} \approx 3-4$ fs.[48]

In the past years, we have engaged ourselves in a systematic study of τ_{FC} for a variety of common biological cofactors based on *ab initio* MD simulations. We considered the TTQ found in MADH and a bacteriopheophytin prosthetic group, which is involved in the ultrafast charge separation in the phototrophic bacterial antennas (Figure 3). We also investigated amino acid residues like tryptophan, tyrosine, or methionine, as well as disulfide bridges, which may be suspected to be involved in multiple hopping[49] or in resonance flickering[50] mechanisms. All these calculations were done in the gas phase to remove, in a

DOI: 10.1021/ar5002796
Acc. Chem. Res. 2015, 48, 1090−1097

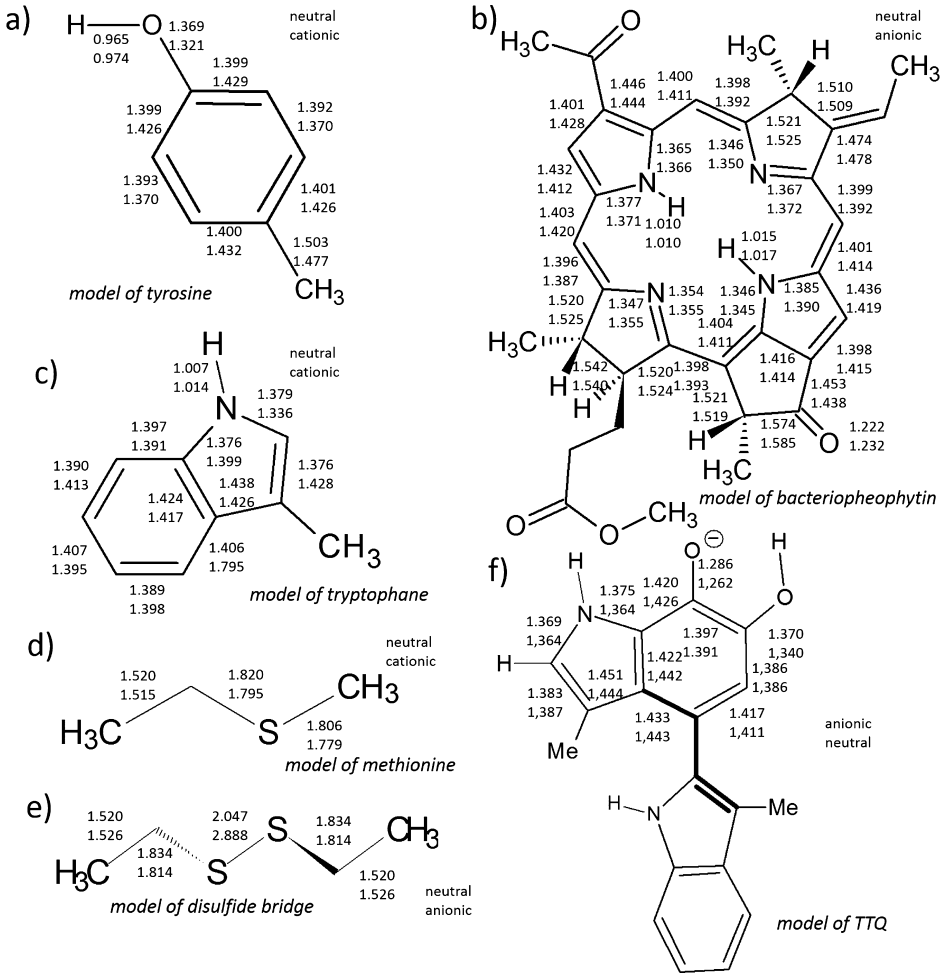

Figure 3. Molecules investigated. The bond lengths were obtained from DFT optimized structures.

first step, the effect of the protein matrices. A detailed analysis for TTQ has been reported in ref 51. Analysis for the other molecules are reported here for the first time (see Supporting Information for detailed additional results).

Our strategy follows Prezhdo and Rossky studies.[42] According to Heller,[52] nuclear wave packet dynamics can be approximated by Gaussian wave packets following semiclassical trajectories. Electronic decoherence triggered by nuclear vibrations (the "bath") is the product of two contributions: decay of nuclear wave packet overlap (J_{ovr}) between the two PESs and dephasing of nuclear wave function (J_{phase}).[42,53] The former is likely to take place faster than the latter and will be the function of our main interest here. J_{ovr} can be evaluated by launching semiclassical MD simulations on the PES corresponding to the two redox states and by evaluating the time-dependent nuclear overlap, J_{ovr}. We refer the reader to ref 42 for the detailed mathematical expressions needed for calculating J_{ovr}. Since the nuclei feel different forces on the two PESs their positions and momenta will diverge over time, and J_{ovr} should irreversibly decay to zero if several nuclei are involved. For each molecule investigated, we carried out several tens of *ab initio* MD simulations. We thereafter report average curves for J_{ovr}.

As seen in Figure 4, the decay of the real part of J_{ovr} takes place within a few femtoseconds. Since the characteristic decay times τ_{ovr} are small, a short time approximation should be valid, and we can identify τ_{FC} to τ_{ovr}. The reorganization energies reflect the coupling between the electronic system and its

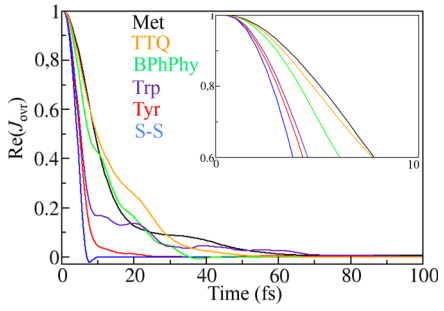

Figure 4. Graph depicting the average bath overlap function for several biological redox fragments taken in the gas phase.

environment (Table 1 and Figure 3). With the exception of the disulfide bridge, very small geometrical variations take place on these cofactors. Yet these small reorganizations do not prevent fast decoherence. In fact, eq 2 only roughly accounts for the trends compiled in Table 1, suggesting that more subtle mechanisms are hidden behind the decay of J_{ovr}.

The deconvolution of J_{ovr} into product of atomic contributions reveals the actual molecular mechanism of electronic decoherence. For TTQ, we found that four atoms defining group 1 (in blue in Figure 5) are the initial contributors to the decay of overlap. However, the decay caused by these atoms alone is not sufficient to induce full decoherence. This is because the variations of bond lengths

DOI: 10.1021/ar5002796
Acc. Chem. Res. 2015, 48, 1090−1097

Table 1. Characteristic Times for the Decay of Bath Overlap for Several Molecules[a]

	τ_{ovr} (fs)	λ (eV)
tyrosine	4.2 (6.9)	0.178
tryptophan	4.5 (8.0)	0.131
methionine	7.6 (10.2)	0.080
bacteriopheophytin	6.0 (8.9)	0.106
disulfide bridge	3.8 (4.9)	0.353
TTQ	7.7 (10.0)	0.084

[a] τ_{ovr} is defined as the time required for J_{ovr} to drop to $e^{-1/2}$ of its initial value (consistent with the Gaussian shape of the function). The values in parentheses are calculated with eq 2 using the reorganization energies evaluated by DFT (OPTX-PBE functional with the TZVP/GEN-A2* basis sets).

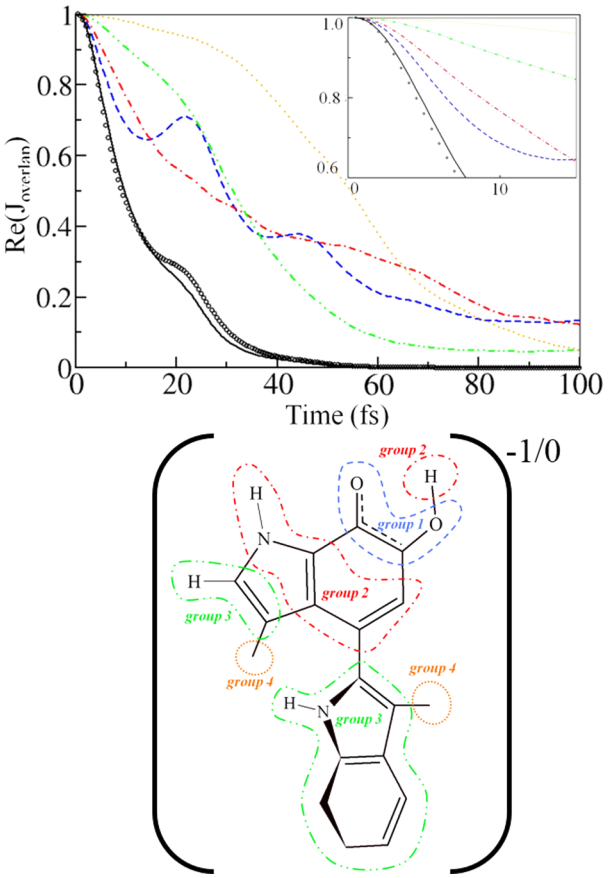

Figure 5. Illustration of the mechanism of the decay of bath overlap in the TTQ cofactor. Adapted with permission from ref 51. Copyright 2013 NRC Research Press.

between atoms of group 1 (0.03 Å) are much smaller than widths of the nuclear wave packet (around 0.1 Å).

The other nuclei contribute to the decay of J_{ovr} but only after a certain delay. The longer the distance from nuclei of group 1, the longer the delay is. Our interpretation is that since nuclei belonging to groups 2−4 are not directly affected by the change of redox state of the molecule, they do not contribute to decoherence in the very short times. However, the nuclei belonging to group 2 are mechanically coupled to those of group 1, through covalent bonds, and finally start to evolve differently on the two PESs after some time. Therefore, overlap decay is the result of the weak contributions of numerous atoms, which taken together lead to its irreversible decay. A similar mechanism is at play for tyrosine, tryptophan, and methionine residues (see Figures S1−S4, Supporting Information). Interestingly even in bacteriopheophytin, which presents the largest aromatic system, overlap decays in a few femtoseconds. The disulfide bridge constitutes a particular case. The decay of J_{ovr} is entirely governed by the divergence of the sulfur atoms as a result of the S−S bond lengthening, which is displaced by 0.8 Å between the two states. This last mechanism should be general for electron transfers inducing the breaking of covalent or hydrogen bonds.[54] In such cases, decoherence is expected to arise in 1−2 fs as a result of the decay of overlap of one vibrational mode. We reported a similar mechanism for a spin-forbidden reaction within a copper−dioxygen complex.[55]

Future work will have to include the environment, which may further contribute to a diminution of τ_{ovr} due to electrostatic interactions with the cofactors.[48] For example, based on classical MD simulations and using a short time approximation to evaluate τ_{FC} (eq 3), Lockwood et al. predicted that water should be an exceptionally effective medium to induce decoherence.[48]

Now, it is possible that the situation may be different in biological systems because of their composite nature and of the secondary and tertiary structures of proteins. At present it is however difficult to see how bath overlap could be slowed in a protein matrix. Some authors suggested that coherences may be preserved in case of weak energy gap fluctuations.[56] Longer coherence times might also be possible for stronger electronic coupling. ET in DNA might be a good candidate. Future simulations will be required to answer these possibilities. Finally, note that investigating how electronic decoherence appears in the condensed phase should also be helpful to improve simulation algorithms for non-Born−Oppenheimer MD, which include decoherence corrections.[57−60]

DEVELOPMENT OF MORE ACCURATE SIMULATION TOOLS

To answer the interrogations as quantitatively as possible, specific simulation tools are required. Toward this end, we

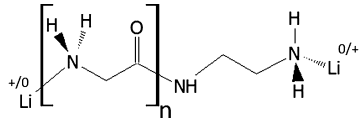

Figure 6. Prototypical model of biological electron transfer. Reproduced with permission from ref 69. Copyright 2012 American Chemical Society.

invested efforts in the constrained DFT (cDFT) method.[61−63] The basic idea of cDFT is to impose a user-defined total charge on specific groups of atoms when solving the Kohn−Sham equations via the self-consistent-field procedure. For an ET process, it is possible to define *ad hoc* diabatic states where the electron to be transferred is localized either on D or on A. cDFT can also, in principle, give access to quantum mechanical estimates of H_{DA}.[64−67] This method relies on the assumption that the Kohn−Sham determinants can be assimilated to the true wave functions. Furthermore, since the determinants are obtained with different Hamiltonians, they are in general not orthogonal and are usually transformed into an appropriate orthogonal basis.[64] We implemented the method in the program deMon2k.[68]

DOI: 10.1021/ar5002796
Acc. Chem. Res. 2015, 48, 1090−1097

Table 2. Decay Times of the High Temperature Franck−Condon Factors (in fs) and Average Electronic Coupling (in cm^{-1}) for Different Donor to Acceptor Distances (in Å)[a]

n	R_{Li-Li}	in the gas phase, τ_{FC}	$\langle H_{DA}\rangle$	R_{Li-Li}	in water, τ_{FC}	$\langle H_{DA}\rangle$
1	10.5	4.16 ± 0.08	29.7 (5.4)	10.5	1.36 ± 0.29	18.2 (3.4)
2	14.0	4.27 ± 0.17	3.92 (2.68)	14.5	1.64 ± 0.05	10.0 (1.8)
3	17.2	4.59 ± 0.21	0.77 (0.29)	16.8	1.56 ± 0.07	1.08 (0.19)
4	20.8	4.54 ± 0.20	0.150 (0.067)	20.9	1.50 ± 0.02	0.100 (0.011)
5	24.1	4.55 ± 0.11	0.013 (0.007)	24.1	1.53 ± 0.12	0.042 (0.002)

[a]The uncertainties correspond to a confidence interval of 95%.[69]

For the sake of illustration, consider an electron transfer between two lithium atoms through a polyglycine peptide of increasing length (Figure 6).[69] cDFT Born−Oppenheimer MD simulations were carried out in the gas phase and in explicit water. The trajectories were biased to visit only the region of degeneracy (by application of a harmonic constraining potential). The average coupling (Table 2) decays from a few tens to a few hundredths of cm^{-1} as expected for an ET along a polypeptide chain. These data are encouraging. More benchmarks will however be needed to better assess the performance of cDFT in capturing subtle quantum effects transpiring through H_{DA} like interferences among multiple pathways.

The Franck−Condon times, τ_{FC}, calculated by eq 3, are found to be independent of the bridge length. On the other hand, the aqueous environment induces a drop of τ_{FC} by a factor of 3. This result is consistent with those of ref 48, where it is predicted that an aqueous environment should contribute efficiently to electronic decoherence. These recently developed tools are currently applied in our group on systems of biological interest.

CONCLUDING REMARKS AND PERSPECTIVES

Our understanding of the interplay between protein dynamics and electron tunneling in proteins greatly increased over the last years, partly thanks to atomistic simulations. In particular, investigations of natural systems have shown how they can cope with the unavoidable structural fluctuations of the biological matter and still sustain efficient tunneling rates. The advent of attosecond spectroscopies in the near future should allow one to follow in real time the flow of electrons from the donor to the acceptor. Theoretical and computational approaches will have to accompany these experimental developments. We proposed, for example, to extend the approach based on the topological analyses of real-space functions like the electronic density or the electron localization function to the time-dependent domain.[70]

The coming years will certainly contribute to bring fascinating new insights on the strategies found by Nature to shuttle electrons in biology. Time might also have come to invest the accumulated knowledge about the subtle effects associated with electron tunneling (interferences, pure dephasing, decoherence, etc.) in the development of innovative strategies for biomimetic catalysts.

ASSOCIATED CONTENT

Supporting Information

Computational protocol for overlap decay, lengths of simulations and number of sets of diverging trajectories for the calculation of average curve J_{ovr}, and bath overlap decay in models of methionine, disulfide bridge, tyrosine, and bacteriopheophytin in vacuum. This material is available free of charge via the Internet at http://pubs.acs.org.

AUTHOR INFORMATION

Corresponding Author

*E-mail: aurelien.de-la-lande@u-psud.fr.

Notes

The authors declare no competing financial interest.

Biographies

Christophe Narth worked on electronic decoherence in Orsay before moving to Université Pierre et Marie Curie where he is currently preparing a Ph.D. on the development of polarizable force fields.

Natacha Gillet defended her Ph.D. in 2014 at Université Paris Sud. Her work focused on biological electron and proton transfers.

Fabien Cailliez is Associate professor at Université Paris Sud. His research is focused on the study of condensed matter by molecular simulations.

Bernard Lévy is Associate researcher at Université Paris Sud. His main fields of research concern the internal dynamics of proteins: chemical reactions, conformational changes, and nonadiabatic processes.

Aurélien de la Lande is a CNRS staff researcher. His main scientific interests are focused on theoretical investigations of biological electron and proton transfers, including methodological developments.

ACKNOWLEDGMENTS

The authors are grateful to the collaborators who contributed to the results summarized in this Account, in particular I. Demachy, M. Desouter-Lecomte, J. Řezáč, N. Babcock, E. Zahedinejad, P. Müller, K. Brettel, L. Baciou, C. Houée-Lévin, J. Pilmé, D. Salahub, and A. Köster.

REFERENCES

(1) Moser, C. J.; Farid, T. A.; Chobot, S. E.; Dutton, P. L. Electron tunneling chains of mitochondria. *Biochim. Biophys. Acta* **2006**, *1757*, 1096−1109.

(2) Muren, N. B.; Olmon, E. D.; Barton, J. Solution, surface, and single molecule platforms for the study of DNA-mediated charge transport. *Phys. Chem. Chem. Phys.* **2012**, *14*, 13754−13771.

(3) Genereux, J. C.; Boal, A. K.; Barton, J. K. DNA-mediated charge transport in redox sensing and signaling. *J. Am. Chem. Soc.* **2010**, *132*, 891−905.

(4) Migliore, A.; Polizzi, N. F.; Therien, M. J.; Beratan, D. N. Biochemistry and theory of proton-coupled electron transfer. *Chem. Rev.* **2014**, *114*, 3381−3465.

(5) Hammes-Schiffer, S. Introduction: Proton-coupled electron transfer. *Chem. Rev.* **2010**, *110*, 6937−6938.

(6) Newton, M. D. Quantum chemical probes of electron-transfer kinetics: The nature of donor−acceptor interactions. *Chem. Rev.* **1991**, *91*, 767−792.

DOI: 10.1021/ar5002796
Acc. Chem. Res. 2015, 48, 1090−1097

(7) Marcus, R. A.; Sutin, N. Electron transfers in chemistry and biology. *Biochim. Biophys. Acta* **1985**, *811*, 265−322.
(8) King, G.; Warshel, A. Investigation of the free energy functions for electron transfer reactions. *J. Chem. Phys.* **1990**, *93*, 8682−8692.
(9) Blumberger, J. Free energies for biological electron transfer from QM/MM calculation: Method, application and critical assessment. *Phys. Chem. Chem. Phys.* **2008**, *10*, 5651−5667.
(10) McConnell, H. M. Intramolecular charge transfer in aromatic free radicals. *J. Chem. Phys.* **1961**, *35*, 508−515.
(11) Winkler, J. R.; Gray, H. B. Long range electron tunneling. *J. Am. Chem. Soc.* **2014**, *36*, 2930−2939.
(12) Cordes, M.; Giese, B. Electron transfer in peptides and proteins. *Chem. Soc. Rev.* **2009**, *38*, 892−901.
(13) Gray, H. B.; Winkler, J. R. Long range electron transfers. *Proc. Natl. Acad. Soc. U.S.A.* **2005**, *102*, 3534−3539.
(14) Onuchic, J. N.; Beratan, D. N. A predictive theoretical model for electron tunneling pathways in proteins. *J. Chem. Phys.* **1990**, *92*, 722−733.
(15) Stuchebrukhov, A. A. Long distance electron tunneling in proteins. *Theor. Chem. Acc.* **2003**, *110*, 291−306.
(16) Paddon-Row, M. N.; Shephard, M. J. Through-bond orbital coupling, the parity rule, and the design of "superbridges" which exhibit greatly enhanced electronic coupling: A natural bond orbital analysis. *J. Am. Chem. Soc.* **1997**, *119*, 5355−5365.
(17) Prytkova, T. R.; Kurnikov, I. V.; Beratan, D. N. Coupling coherence distinguishes structure sensitivity in protein electron transfer. *Science* **2007**, *315*, 622−625.
(18) Daizadeh, I.; Medvedev, E. S.; Stuchebruhkov, A. A. Effect of protein dynamics on biological electron transfer. *Proc. Natl. Acad. Soc. U.S.A.* **1997**, *94*, 3703−3708.
(19) Wolfgang, J.; Risser, S. M.; Priyadarshy, S.; Beratan, D. N. Secondary structure conformations and long range electronic interactions in oligopeptides. *J. Phys. Chem. B* **1997**, *101*, 2986−2991.
(20) Balabin, I. A.; Beratan, D. N.; Skourtis, S. S. Persistence of structure over fluctuations in biological electron-transfer reactions. *Phys. Rev. Lett.* **2008**, *101*, No. 158102.
(21) Troisi, A.; Ratner, M. A.; Zimmt, M. B. Dynamic nature of the intramolecular electronic coupling mediated by a solvent molecule: A computational study. *J. Am. Chem. Soc.* **2004**, *126*, 2215−2224.
(22) Kawatsu, T.; Kakitani, T.; Yamato, T. Destructive interference in the electron tunneling through protein media. *J. Phys. Chem. B* **2002**, *106*, 11356−11366.
(23) Prytkova, T. R.; Kurnikov, I. V.; Beratan, D. N. Ab initio based calculations of electron-transfer rates in metalloproteins. *J. Phys. Chem. B* **2005**, *109*, 1618−1625.
(24) Migliore, A.; Corni, S.; Di Felice, R.; Molinari, R. Water-mediated electron transfer between protein redox centers. *J. Phys. Chem. B* **2007**, *111*, 3774−3781.
(25) de la Lande, A.; Parisel, O.; Moliner, V. Long distance electron-transfer mechanism in peptidylglycine α-hydroxylating monooxygenase: A perfect fitting for a water bridge. *J. Am. Chem. Soc.* **2007**, *129*, 11700−11707.
(26) Melia, C.; Ferrer, S.; Řezáč, J.; Parisel, O.; Reinaud, O.; Moliner, V.; de la Lande, A. Investigation of the hydroxylation mechanism of non-coupled copper oxygenases by ab initio molecular dynamics simulations. *Chem.—Eur. J.* **2013**, *19*, 17328−17337.
(27) El Hammi, E.; Houée-Lévin, C.; Řezáč, J.; Lévy, B.; Demachy, I.; Baciou, L.; de la Lande, A. New insights into the mechanism of electron transfer within flavohemoglobins: Tunneling pathways, packing density, thermodynamic and kinetic analyses. *Phys. Chem. Chem. Phys.* **2012**, *14*, 13872−13880.
(28) Cailliez, F.; Müller, P.; Gallois, M.; de la Lande, A. ATP binding and aspartate protonation enhance photoinduced electron transfer in plant cryptochrome. *J. Am. Chem. Soc.* **2014**, *136*, 12974−12986.
(29) de la Lande, A.; Babcock, N.; Řezáč, J.; Sanders, B. C.; Salahub, D. R. Surface residues dynamically organize water bridges to enhance electron transfer between proteins. *Proc. Natl. Acad. Sci. U. S. A.* **2010**, *107*, 11799−11804.
(30) Davidson, V. L. Protein control of true, gated, and coupled electron transfer reactions. *Acc. Chem. Res.* **2008**, *41*, 730−738.
(31) Ma, J. K.; Wang, Y.; Carrell, C. J.; Mathews, F. S.; Davidson, V. L. A single methionine residue dictates the kinetic mechanism of interprotein electron transfer from methylamine dehydrogenase to amicyanin. *Biochemistry* **2007**, *46*, 11137−11146.
(32) Chaves, I.; Pokorny, R.; Byrdin, M.; Hoang, N.; Ritz, T.; Brettel, K.; Essen, L.-O.; van der Horst, G. T. J.; Batschauer, A.; Ahmad, M. The cryptochromes: Blue light photoreceptors in plants and animals. *Annu. Rev. Plant Biol.* **2011**, *62*, 335−364.
(33) Immeln, D.; Weigel, A.; Kottke, T.; Pérez Lustres, J.-L. Primary events in the blue light sensor plant cryptochrome: Intraprotein electron and proton transfer revealed by femtosecond spectroscopy. *J. Am. Chem. Soc.* **2012**, *134*, 12536−12546.
(34) Müller, P.; Bouly, J.-P.; Hitomi, K.; Balland, V.; Getzoff, E. D.; Ritz, T.; Brettel, K. ATP binding turns plant cryptochrome into an efficient natural photoswitch. *Sci. Rep.* **2014**, *4*, No. 5175.
(35) Keinan, S.; Nocek, J. M.; Hoffman, B. M.; Beratan, D. N. Interfacial hydration, dynamics and electron transfer: Multi-scale ET modeling of the transient [myoglobin, cytochrome b5] complex. *Phys. Chem. Chem. Phys.* **2012**, *14*, 13881−13889.
(36) Breuer, M.; Rosso, K. M.; Blumberger, J. Electron flow in multiheme bacterial cytochromes is a balancing act between heme electronic interaction and redox potentials. *Proc. Natl. Acad. Sci. U.S.A.* **2014**, *111*, 611−616.
(37) Balabin, I. A.; Onuchic, J. N. Dynamically controlled protein tunneling paths in photosynthetic reaction centers. *Science* **2000**, *290*, 114−117.
(38) Beratan, D. N.; Skourtis, S. S.; Balabin, I. A.; Balaeff, A.; Keinan, S.; Venkatramani, R.; Xiao, R. Steering electrons on moving pathways. *Acc. Chem. Res.* **2009**, *42*, 1669−1678.
(39) Onuchi, J. N.; Wolynes, P. G. Classical and quantum picture of reaction dynamics in condensed matter: Resonances, dephasing, and all that. *J. Phys. Chem.* **1988**, *92*, 6495−6503.
(40) Skourtis, S. S.; Waldeck, D. H.; Beratan, D. N. Fluctuations in biological and bioinspired electron-transfer reactions. *Annu. Rev. Phys. Chem.* **2010**, *61*, 461−485.
(41) Bialek, W.; Bruno, W. J.; Joseph, J.; Onuchic, J. N. Quantum and classical dynamics in biochemical reactions. *Photosynth. Res.* **1989**, *22*, 15−27.
(42) Prezhdo, O. V.; Rossky, P. J. Evaluation of quantum transition rates from quantum-classical molecular dynamics simulations. *J. Chem. Phys.* **1997**, *107*, 5863−5878.
(43) Hwang, H.; Rossky, P. G. Electronic decoherence induced by intramolecular vibrational motions in a betaine dye molecule. *J. Phys. Chem. B* **2004**, *108*, 6723−6732.
(44) Troisi, A.; Nitzan, A.; Ratner, M. A. A rate constant expression for charge transfer through fluctuating bridges. *J. Chem. Phys.* **2003**, *119*, 5782−5788.
(45) Nishioka, H.; Kimura, A.; Yamato, K.; Kawatsu, T.; Kakitani, T. Interference, fluctuation, and alternation of electron tunneling in protein media. 2. Non-Condon theory for the energy gap dependence of electron transfer rate. *J. Phys. Chem. B* **2005**, *109*, 15621−15635.
(46) Tanaka, S.; Starikov, E. B. Analysis of electron-transfer rate constant in condensed media with inclusion of inelastic tunneling and nuclear quantum effects. *Phys. Rev. E* **2010**, *81*, No. 027101.
(47) Skourtis, S. S.; Balabin, I. A.; Kawatsu, T.; Beratan, D. N. Protein dynamics and electron transfer: Electronic decoherence and non-Condon effects. *Proc. Natl. Acad. Sci. U.S.A.* **2005**, *102*, 3552−3557.
(48) Lockwood, D. M.; Cheng, Y.-K.; Rossky, P. J. Electronic decoherence for electron transfer in blue copper proteins. *Chem. Phys. Lett.* **2001**, *345*, 159−165.
(49) Warren, J. J.; Ener, M. E.; Vlček, A., Jr.; Winkler, J. R.; Gray, H. B. Electron hopping through protein. *Coord. Chem. Rev.* **2012**, *256*, 2478−2487.
(50) Zhang, Y.; Liu, C.; Balaeff, A.; Skourtis, S. S.; Beratan, D. N. Biological charge transfer via flickering resonance. *Proc. Natl. Acad. Sci. U.S.A.* **2014**, *111*, 10049−10054.

DOI: 10.1021/ar5002796
Acc. Chem. Res. 2015, 48, 1090−1097

(51) Narth, C.; Gillet, N.; Lévy, B.; Demachy, I.; de la Lande, A. Investigation of the molecular mechanisms of electronic decoherence within a quinone cofactor. *Can. J. Chem.* **2013**, *91*, 628−636.
(52) Heller, E. J. Frozen Gaussians: A very simple semiclassical approximation. *J. Chem. Phys.* **1981**, *75*, 2923−2931.
(53) Fiete, G. A.; Heller, E. J. Semiclassical theory of coherence and decoherence. *Phys. Rev. A* **2003**, *68*, No. 022112.
(54) Costentin, C.; Robert, M.; Savéant, J.-M.; Tard, C. Breaking bonds with electrons and protons. Models and examples. *Acc. Chem. Res.* **2014**, *47*, 271−280.
(55) de la Lande, A.; Řezáč, J.; Lévy, B.; Sanders, B. C.; Salahub, D. R. Transmission coefficients for chemical reactions with multiple states: Role of quantum decoherence. *J. Am. Chem. Soc.* **2011**, *133*, 3883−3894.
(56) Akimov, A. V.; Prezhdo, O. V. Persistent electronic coherence despite rapid loss of electron−nuclear correlation. *J. Phys. Chem. Lett.* **2013**, *4*, 3857−3864.
(57) Fang, J. Y.; Hammes-Schiffer, S. Improvement of the internal consistency in trajectory surface hopping. *J. Phys. Chem. A* **1999**, *103*, 9399−9407.
(58) Jasper, A. W.; Zhu, C.; Nangia, S.; Truhlar, D. G. Introductory lecture: Nonadiabatic effects in chemical dynamics. *Faraday Discuss.* **2004**, *127*, 1−22.
(59) Granucci, G.; Persico, M.; Zoccante, A. Including quantum decoherence in surface hopping. *J. Chem. Phys.* **2010**, *133*, No. 134111.
(60) Shenvi, N.; Subotnik, J. E.; Yang, W. Simultaneous-trajectory surface hopping: A parameter-free algorithm for implementing decoherence in nonadiabatic dynamics. *J. Chem. Phys.* **2011**, *134*, No. 144102.
(61) Dederichs, P. H.; Blügle, S.; Zeller, R.; Akai, H. Ground states of constrained systems: Application to cerium impurities. *Phys. Rev. Lett.* **1984**, *53*, 2512−2515.
(62) Kaduk, B.; Kowalczyk, T.; Van Voorhis, T. Constrained density functional theory. *Chem. Rev.* **2012**, *112*, 321−370.
(63) Wu, Q.; Van Voorhis, T. Direct optimization method to study constrained systems within density-functional theory. *Phys. Rev.* **2005**, *72*, No. 024502.
(64) Wu, Q.; Van Voorhis, T. Extracting electron transfer coupling elements from constrained density functional theory. *J. Chem. Phys.* **2006**, *125*, No. 164105.
(65) Hoberhofer, H.; Blumberger, J. Electronic coupling matrix elements from charge constrained density functional theory calculations using a plane wave basis set. *J. Chem. Phys.* **2010**, *133*, No. 244105.
(66) de la Lande, A.; Salahub, D. R. Derivation of interpretative models for long range electron transfer from constrained density functional theory. *THEOCHEM.* **2010**, *943*, 115−120.
(67) Kubas, A.; Hoffmann, F.; Heck, A.; Oberhofer, H.; Elstner, M.; Blumberger, J. Electronic couplings for molecular charge transfer: Benchmarking CDFT, FODFT, and FODFTB against high-level ab initio calculations. *J. Chem. Phys.* **2014**, *140*, No. 104105.
(68) Geudtner, G.; Calaminici, P.; Carmona-Espindola, J.; del Campo, J. M.; Dominguez-Soria, V. D.; Flores-Moreno, R.; Gamboa, G. U.; Goursot, A.; Köster, A. M.; Reveles, J. U.; Tzonka, M.; Vasquez-Perez, J. M.; Vela, A.; Zúñinga-Gutierrez, B.; Salahub, D. R. deMon2k. *Wiley Interdiscip. Rev.: Comput. Mol. Sci.* **2012**, *2*, 548−555.
(69) Řezáč, J.; Lévy, B.; Demachy, I.; de la Lande, A. Robust and efficient constrained DFT molecular dynamics approach for biochemical modeling. *J. Chem. Theory Comput.* **2012**, *8*, 418−427.
(70) Pilmé, J.; Luppi, E.; Bergès, J.; Houée-Lévin, C.; de la Lande, A. Topological analysis of time-dependent electronic structures: Application to electron-transfers in methionine encephalin. *J. Mol. Model.* **2014**, *10*, 2368−2381.

DOI: 10.1021/ar5002796
Acc. Chem. Res. 2015, 48, 1090−1097